

Passive Vacuum Solar Flash Desalination

Mohammad Abutayeh

Dept. of Chemical Engineering, University of South Florida, Tampa, FL 33620, USA

D. Yogi Goswami

Clean Energy Research Center, University of South Florida, Tampa, FL 33620, USA

DOI 10.1002/aic.12060

Published online October 19, 2009 in Wiley InterScience (www.interscience.wiley.com).

A model for a sustainable desalination process has been developed. The simulated process consists of pumping seawater through a solar heater before flashing it under a passively created vacuum in an elevated chamber. The vacuum enhances evaporation and is maintained by the balance between the hydrostatic pressure inside the elevated flash chamber and the atmospheric pressure. The developed model uses theoretical thermodynamic relations to describe the process setting it apart from previous empirical correlations. © 2009 American Institute of Chemical Engineers *AIChE J.* 56: 1196–1203, 2010

Keywords: desalination, flash desalination, solar desalination

Introduction

The fresh water demand is persistently increasing as populations around the world keep growing and as existing fresh water reserves keep declining because of consumption and pollution. Marine waters represent an infinite water source because almost 98% of global water is present in oceans; therefore, desalination is the logical approach to meet the rising fresh water demand.

The energy demand is continually increasing because of the relentless global industrialization. Oil and gas remain the principal source of energy for most of the world; however, their reserves are dwindling, their production is peaking, and their consumption is harming the environment. Serious economic and social disruptions are unfolding over those finite energy resources; hence, using renewable energy resources will help avoid catastrophic conflicts, continue modern lifestyles, and preserve an increasingly warming and polluting environment. Solar radiation is a very appealing source of energy because it is available at no cost; furthermore, exploiting it has no notable adverse effect on the environment. Plenty of research and development have been undertaken to better utilize this free form of energy to develop more efficient and sustainable processes, such as water desalination and power generation.¹

Reducing the pressure above the surface of liquids enhances their evaporation. This phenomenon can be integrated into a continuous desalination process by flashing seawater in a vacuumed chamber to produce water vapor that is condensed producing fresh water. Gravity can be used to balance the hydrostatic pressure inside the elevated flash chamber with the outdoor atmospheric pressure to maintain that vacuum, while low-grade solar radiation can be used to heat seawater before flashing.

The objective of this study is to simulate a solar flash desalination process under a hydrostatically sustained vacuum and analyze its controlling variables. Simulation is achieved with a rigorous model built to depict the proposed unit by using the fundamental physical and thermodynamic relationships to describe the process. The model is complemented by reliable empirical correlations to estimate the physical properties of the involved species and the operational parameters of the proposed system needed to perform accurate mass and energy balances. This approach is scientifically more valid than exclusive empirical methods and will increase the applicability of the developed model.

Background

Low-grade solar heat desalination under passive vacuum was devised and simulated theoretically and experimentally by Al-Kharabsheh and Goswami.² A simplified process flow diagram of their desalination process is shown in Figure 1.

Correspondence concerning this article should be addressed to D. Y. Goswami at goswami@eng.usf.edu

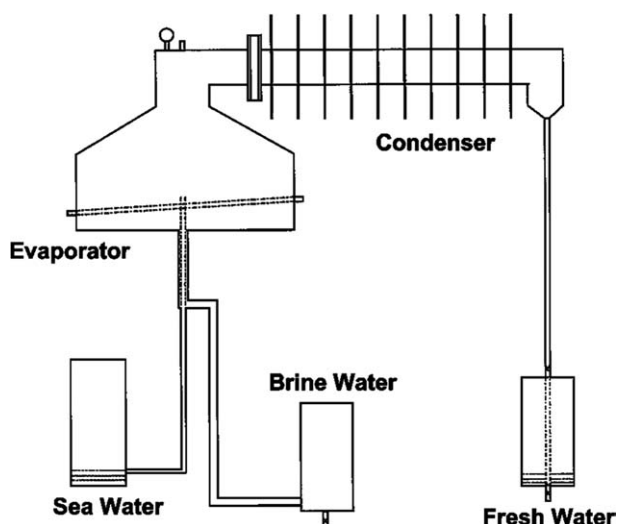


Figure 1. Passive vacuum desalination system.

Atmospheric pressure moves cool seawater from a ground level tank into an elevated vacuumed evaporator through an injection pipe, where water starts to evaporate due to solar or other low-grade heat supplied to the chamber. The concentrated brine is then withdrawn through a withdrawal pipe annulus to the injection pipe to recover heat, while the vapor moves toward a condenser because of a vapor pressure gradient through a finned pipe. Vapor then condenses by losing its latent heat of condensation to the ambient and flows down to a ground level tank due to gravity. The vacuum is naturally maintained by the hydrostatic balance between all of the connected vessels and the atmospheric pressure.

The experimental results of Al-Kharabsheh and Goswami matched well with the predictions of their developed model³; however, the model was largely empirical, thus limiting its applicability. In addition, the size of the evaporator of the desalination unit had to be very large to produce a practical output.

The above desalination system was later modified by Maroo⁴ to overcome the big size and the large level fluctuations of the evaporator. A simplified process flow diagram of the modified desalination process is shown in Figure 2.

Seawater is pumped through a condenser to preheat it before it enters a solar heater and then flashes into a passively vacuumed evaporator through an expansion orifice producing water vapor and concentrated brine. The flashed vapor then moves toward the condenser due to a vapor pressure gradient and condenses by losing its latent heat of condensation to the entering seawater in the condenser. The condensate and the concentrated brine flow down to ground level tanks by gravity, while the vacuum is naturally sustained by the hydrostatic balance between all of the connected vessels and the atmospheric pressure.

Single and double-stage configurations were simulated; however, the model was largely empirical, which limited its applicability. In particular, no fundamental thermodynamic relations were used to characterize the flashing process, which is the most fundamental operation of the entire desalination system.

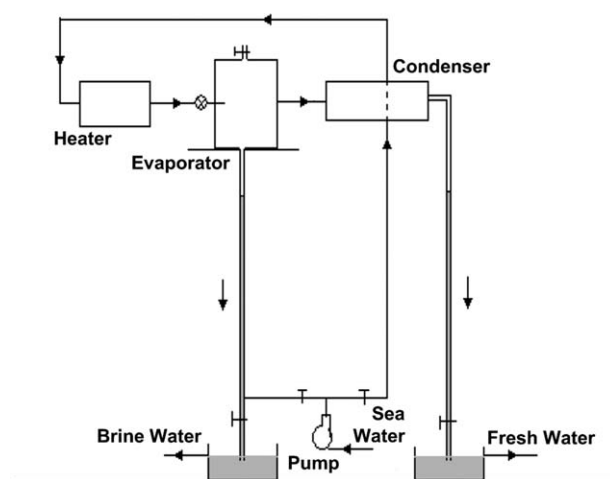


Figure 2. Passive vacuum flash desalination system.

Schematics

The proposed passive vacuum solar flash desalination system consists of a saline water tank, a concentrated brine tank, and a fresh water tank placed on ground level plus an evaporator and a condenser located at least 10 m above ground, as shown in Figure 3. The ground level tanks are open to the atmosphere, whereas the evaporator–condenser assembly, or flash chamber, is insulated and sealed to retain both heat and vacuum.

The process begins by pumping the flash chamber with seawater while its top valves are open and its bottom ones are closed until it is completely filled with water and free of air. The valve positions of the flash chamber are then switched around to let the water drop under gravity creating the desired vacuum without a vacuum pump.

In a continuous operation, cool saline water is pumped through a condenser to preheat it before it enters a solar heater and then flashes into a vacuumed evaporator through an expansion orifice producing water vapor and concentrated brine. The water vapor then moves toward the condenser due to a vapor pressure gradient

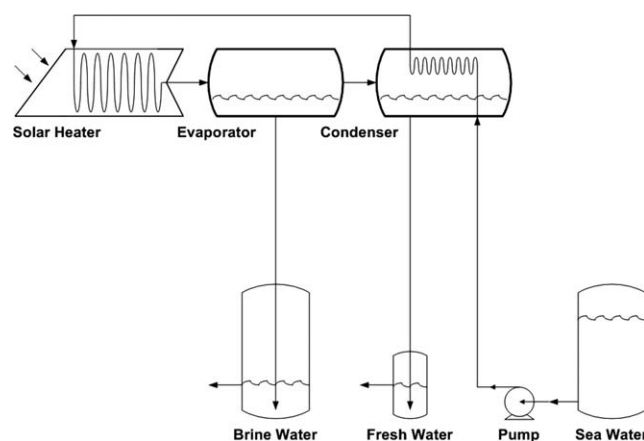


Figure 3. Proposed desalination system.

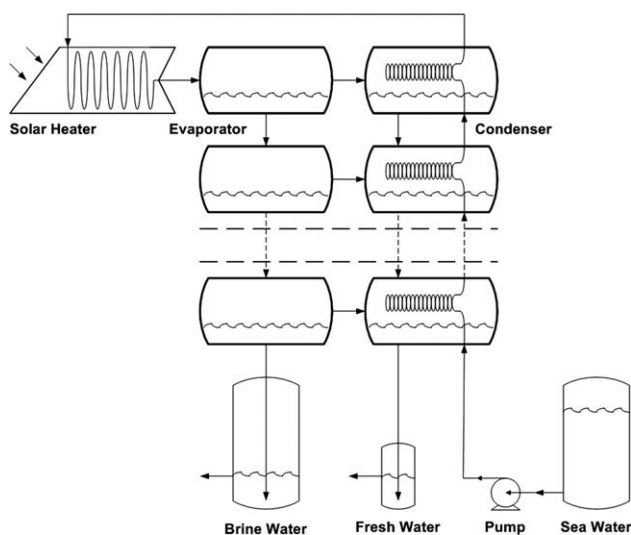


Figure 4. Multistage configuration of the proposed desalination system.

and condenses by losing its latent heat of condensation to the entering saline water. The condensate and the concentrated brine flow down to a fresh water and a brine water tanks, respectively, due to gravity through discharge pipes. Each of the fresh water and the brine water tanks have a discharge pipe located a few centimeters above the level of the inlet water pipes keeping their levels constant to hydrostatically maintain the vacuum in the flash chamber in addition to retrieving the fresh water product and rejecting the concentrating brine.

Multistage solar flash desalination can be implemented by flashing saline water in sequentially lower pressure flash chambers, as shown in Figure 4. Applying the multistage strategy to solar flash desalination will result in more evaporation and better recovery of the heat of condensation resulting in more fresh water output.

Model

The following model is built to depict the continuous desalination process outlined above in Figure 3 to analyze the controlling variables of the fresh water output of the proposed desalination unit. The model assumes a quasi-steady-state operation accounting for the build up of noncondensable gases in the flash chamber.

Salt balances around the transitional process equipment are given by:

$$\phi_S \cdot M_S = \phi_P \cdot M_P \quad (1)$$

$$\phi_P \cdot M_P = \phi_X \cdot M_X \quad (2)$$

$$\phi_X \cdot M_X = \phi_H \cdot M_H \quad (3)$$

$$\phi_H \cdot M_H = \phi_W \cdot M_W \quad (4)$$

Overall energy balances around the transitional process equipment are given by:

$$Q_P - W_P + E_P^{\text{in}} - E_P^{\text{out}} = 0 \quad (5)$$

$$Q_C - W_C + E_C^{\text{in}} - E_C^{\text{out}} = E_C^a \quad (6)$$

$$Q_H - W_H + E_H^{\text{in}} - E_H^{\text{out}} = 0 \quad (7)$$

$$Q_E - W_E + E_E^{\text{in}} - E_E^{\text{out}} = 0 \quad (8)$$

Energy inputs to the transitional process equipment are given by:

$$E_P^{\text{in}} = M_S \cdot H_S \quad (9)$$

$$E_C^{\text{in}} = M_P \cdot H_P + M_E \cdot (H_E + H_E^L) \quad (10)$$

$$E_H^{\text{in}} = M_X \cdot H_X \quad (11)$$

$$E_E^{\text{in}} = M_H \cdot H_H \quad (12)$$

Energy outputs from the transitional process equipment are given by:

$$E_P^{\text{out}} = M_P \cdot H_P \quad (13)$$

$$E_C^{\text{out}} = M_X \cdot H_X + M_C \cdot H_C \quad (14)$$

$$E_H^{\text{out}} = M_H \cdot H_H \quad (15)$$

$$E_E^{\text{out}} = M_E \cdot (H_E + H_E^L) + M_W \cdot H_W \quad (16)$$

Energy accumulation in the condenser is given by:

$$E_C^a = M_C^a \cdot H_C^a \quad (17)$$

Adding heat to seawater before flashing is accomplished by a solar heater. The heater consists of single-glazed flat-plate solar collectors directly heating seawater flowing through their absorbing tubes. Solar insolation is geographically referenced and continually varying because of the dynamic solar angles. In addition, solar insolation incident on the collector varies with plate geometry, sky clearness, ground reflectivity, and other factors. Average values for a generic single-glazed flat-plate solar collector will be used to simplify the comparison between the different simulation scenarios. The solar insolation area needed to meet the required heating load can be found using the Hottel–Whillier–Bliss equation⁵:

$$A_{\text{SC}} = \frac{Q_H}{F_R \cdot [\tau \cdot \alpha \cdot I - U \cdot (T_X - T_A)]} \quad (18)$$

Solar heating is usually accomplished indirectly by an intermediary heat exchanger that transfers heat from a solar collector loop to a process loop. The proposed desalination system drops this intermediary heat exchanger by flowing seawater directly through the absorbing tubes of the solar collector; therefore, increasing the efficiency and reducing the cost of the solar heater. On the other hand, this direct heating scheme has its drawback by increasing the risk of corrosion and scale formation causing equipment damage and inhibiting heat transfer. Hermann–Koschikowski–Rommel⁶ developed corrosion-free solar collectors for use in thermal desalination systems composed of series of coated

glass tubes mounted inside a conventional flat-plate solar collector enclosure.

Seawater is a solution of many salts and contains a small amount of dissolved gases. To simplify calculations, seawater salt will be treated as one substance with nitrogen, oxygen, argon, and carbon dioxide making up the dissolved gases.

The average molecular weight of seawater salt can be estimated by considering its major components⁷ as follows

$$\frac{1}{MW_{\text{Salt}}} = \frac{\omega_{\text{Cl}}}{MW_{\text{Cl}}} + \frac{\omega_{\text{Na}}}{MW_{\text{Na}}} + \frac{\omega_{\text{SO}_4}}{MW_{\text{SO}_4}} + \frac{\omega_{\text{Mg}}}{MW_{\text{Mg}}} + \frac{\omega_{\text{Ca}}}{MW_{\text{Ca}}} + \frac{\omega_{\text{K}}}{MW_{\text{K}}} + \frac{\omega_{\text{HCO}_3}}{MW_{\text{HCO}_3}} + \frac{\omega_{\text{Br}}}{MW_{\text{Br}}} + \frac{\omega_{\text{BO}_3}}{MW_{\text{BO}_3}} + \frac{\omega_{\text{Sr}}}{MW_{\text{Sr}}} + \frac{\omega_{\text{F}}}{MW_{\text{F}}} \quad (19)$$

The average molecular weight of streams around the flash chamber can be estimated by considering their major components as follows:

$$MW_{\text{H}} = z_{\text{N}_2} \cdot MW_{\text{N}_2} + z_{\text{O}_2} \cdot MW_{\text{O}_2} + z_{\text{Ar}} \cdot MW_{\text{Ar}} + z_{\text{CO}_2} \cdot MW_{\text{CO}_2} + z_{\text{Salt}} \cdot MW_{\text{Salt}} + z_{\text{H}_2\text{O}} \cdot MW_{\text{H}_2\text{O}} \quad (20)$$

$$MW_{\text{E}} = y_{\text{N}_2} \cdot MW_{\text{N}_2} + y_{\text{O}_2} \cdot MW_{\text{O}_2} + y_{\text{Ar}} \cdot MW_{\text{Ar}} + y_{\text{CO}_2} \cdot MW_{\text{CO}_2} + y_{\text{H}_2\text{O}} \cdot MW_{\text{H}_2\text{O}} \quad (21)$$

$$MW_{\text{W}} = x_{\text{N}_2} \cdot MW_{\text{N}_2} + x_{\text{O}_2} \cdot MW_{\text{O}_2} + x_{\text{Ar}} \cdot MW_{\text{Ar}} + x_{\text{CO}_2} \cdot MW_{\text{CO}_2} + x_{\text{Salt}} \cdot MW_{\text{Salt}} + x_{\text{H}_2\text{O}} \cdot MW_{\text{H}_2\text{O}} \quad (22)$$

$$MW_{\text{C}} = v_{\text{N}_2} \cdot MW_{\text{N}_2} + v_{\text{O}_2} \cdot MW_{\text{O}_2} + v_{\text{Ar}} \cdot MW_{\text{Ar}} + v_{\text{CO}_2} \cdot MW_{\text{CO}_2} + v_{\text{H}_2\text{O}} \cdot MW_{\text{H}_2\text{O}} \quad (23)$$

The gas and salt content of process streams is assumed to be constant before flashing

$$MW_{\text{S}} = MW_{\text{P}} = MW_{\text{X}} = MW_{\text{H}} \quad (24)$$

$$\phi_{\text{S}} = \phi_{\text{P}} = \phi_{\text{X}} = \phi_{\text{H}} \quad (25)$$

The distribution of noncondensable gases between the flashed vapor, the concentrated brine, and the condensed water in the flash chamber can be estimated by assuming equilibrium between the three phases. Salt is considered non-volatile and therefore is not present in the flashed vapor or condensed water streams. Henry's constants for the noncondensable gases and the saturation pressure of water are needed to describe this assumed equilibrium.

Henry's constants for the noncondensable gases are given by⁸:

$$HC_i = HC_i^0 \cdot \exp \left[-HF_i \cdot \left(\frac{1}{T + 273.15} - \frac{1}{298.15} \right) \right] \quad (26)$$

The saturation pressure of water is given by⁹:

$$P_{\text{H}_2\text{O}}^{\text{sat}} = \exp \left[PA - \left(\frac{PB}{T + PC} \right) \right] \quad (27)$$

The vapor-liquid equilibrium distribution coefficient of species *i* is defined as $K_i = y_i/x_i = P_i^{\text{sat}}/P$, and it is widely

Table 1. Equilibrium Parameters

	HC°	HF	PA	PB	PC	α
N ₂	8067573	-3546				1.21
O ₂	358815	-2209				1.22
Ar	384073	-2308				1.23
CO ₂	10915	-445				1.17
H ₂ O			12.76	4391	245	0.98

used to determine the distribution of chemicals between phases in equilibrium.¹⁰ Vapor-liquid equilibrium distribution coefficients are also known as partition coefficients in literature or simply as *K*-values. The *K*-value of salt is zero because of its nonvolatility and the *K*-values of the noncondensable gases can be approximated as follows:

$$K_i = \frac{y_i}{x_i} = \frac{P_i}{P_v} = \frac{HC_i \cdot x_i}{P_v} = \frac{HC_i}{P_v} \quad (28)$$

The *K*-value of water is given by

$$K_{\text{H}_2\text{O}} = \frac{P_{\text{H}_2\text{O}}^{\text{sat}}}{P_v} \quad (29)$$

The vapor-liquid equilibrium distribution coefficients were obtained using SUPERTRAPPTM, a computer code distributed by National Institute of Standards and Technology that calculates the thermodynamic properties of mixtures based on the Peng-Robinson equation of state (EOS). It was used to perform isobaric phase equilibria flash calculations at various temperatures to produce vapor-liquid equilibrium distribution coefficient data. Least squares regression was then used to fit the produced data to the above equilibrium equations by manipulating the values of HC_i^0 , HF_i , PA , PB , and PC . SUPERTRAPPTM simulations are fresh water-based and no salts are included in its flash calculations. To adjust the calculations for saline water, the *K*-values are multiplied by a correction factor, which can be defined as α_i = solubility in fresh water/solubility in seawater for solutes and $\alpha_{\text{H}_2\text{O}}$ = seawater saturation pressure/fresh water saturation pressure for water. The correction factor is a single constant obtained by averaging literature solubility data given over the operating temperature range to simplify calculations.¹¹ Table 1 summarizes the generated equilibrium parameters used in this model.

Two sets of *K*-values are used in this model. One set is evaluated for the evaporator at a specified temperature and is used in flash calculations. The other set is designated for the condenser and is used to solve for the temperature of the condensed water needed to establish equilibrium with the vapor. Flash calculations can now be carried out using the Rachford-Rice equation.¹²

The molar composition of the stream entering the flash chamber is needed to proceed with the flash calculations and can be calculated from the average composition of seawater reported on mass basis⁷ as follows:

$$z_i = \frac{\frac{\phi_i}{MW_i}}{\sum_{\text{All}} \frac{\phi}{MW}} \quad (30)$$

The molar composition of the concentrated brine is given by:

$$x_i = \frac{z_i \cdot N_H}{N_W + N_E \cdot \alpha_i \cdot K_i^E} \quad (31)$$

Similarly, the molar composition of the flashed vapor is given by:

$$y_i = x_i \cdot \alpha_i \cdot K_i^E \quad (32)$$

The molar composition of the condensed water in the condenser can be determined by:

$$v_i = \frac{y_i}{K_i^C} \quad (33)$$

The operating pressure inside the flash chamber has to be between the dew point and the bubble point to carry out a successful flash separation. The dew point and the bubble point pressures are estimated by:

$$\frac{P_{BP}}{P_V} = \sum z_i \cdot \alpha_i \cdot K_i^E \quad (34)$$

$$\frac{P_V}{P_{DP}} = \sum \frac{z_i}{\alpha_i \cdot K_i^E} \quad (35)$$

The low vacuum pressure marginalizes the effect of molecular size, and the fairly high flash temperature weakens the relative importance of intermolecular attractions. As a consequence, the ideal gas law becomes a suitable EOS to express the rising vacuum pressure inside the flash chamber as follows:

$$P_V = \frac{P_V^i \cdot V_V^i + R \cdot (T_E + 273.15) \cdot \int (N_C^a) d\theta}{V_V} \quad (36)$$

The initial vacuum pressure will be assumed equal to the vapor pressure of water at the flash temperature and will be evaluated using the above given saturation pressure relation. The initial vacuum volume can be determined from the geometry of the system and the initial tank levels. The hydrostatic balance relations between the pressure inside the flash chamber and the atmospheric pressure determine the dynamic tank levels allowing for the calculation of the dynamic vacuum volume. The hydrostatic balance relations are written using Bernoulli's fluid equation,¹³ and correlations for stream pressure drop⁹ are included as well. The integral part can be numerically evaluated as time is an input variable.

Summation of fractions are included to complete the flash calculations

$$\sum \phi_i = \sum z_i = \sum x_i = \sum y_i = \sum v_i = 1. \quad (37)$$

The vapor pressure of seawater is 1.84% lower than that of pure water at the same temperature because of the nonvolatile salts and, therefore, the boiling point of seawater is slightly higher than that of fresh water. This phenomenon is known as the boiling point elevation or the vapor pressure depression. Boiling point elevation is a function of salinity and does not depend on the properties of the solute or the solvent.¹⁴

The temperature of seawater drops upon entering the flash chamber to attain equilibrium; however, equilibrium is not

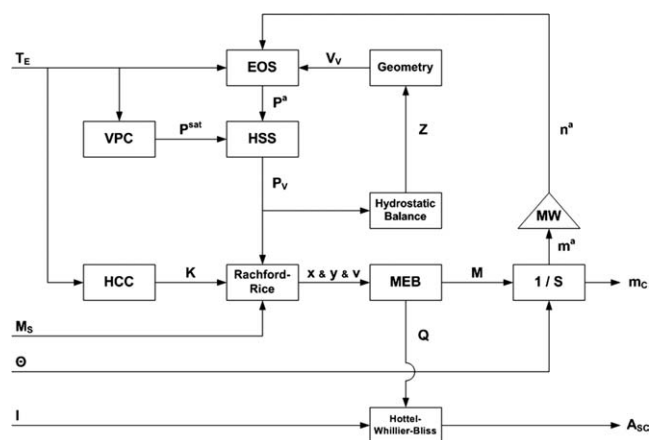


Figure 5. Solution algorithm.

always fully achieved. This phenomenon is known as the nonequilibrium allowance, and it depends on several factors such as flash temperature, flow rates, concentrated brine depth, and chamber geometry.

Correlations for boiling point elevation¹⁵ and nonequilibrium allowance¹⁶ are incorporated into the model as follows:

$$T_W = T_E + \text{BPE} + \text{NEA} \quad (38)$$

$$\begin{aligned} \text{BPE} &= 8.77 \cdot \phi_H \\ &\times (95.76 \cdot 10^{-2} + 81.89 \cdot 10^{-4} \cdot T_E + 16.47 \cdot 10^{-6} \cdot T_E^2) - 0.05 \end{aligned} \quad (39)$$

$$\text{NEA} = \frac{33 \cdot (T_H - T_E)^{0.55}}{T_E - \text{BPE}} \quad (40)$$

A quasi-steady-state operation is assumed to account for the accumulation of noncondensable gases in the flash chamber. This is accomplished by including the accumulation rate in the total mole balance around the flash chamber

$$N_H = N_E + N_W \quad (41)$$

$$N_E = N_C + N_C^a \quad (42)$$

$$M_E = M_C + M_C^a \quad (43)$$

Assuming total condensation of the flashed water vapor

$$v_{H_2O} \cdot N_C = y_{H_2O} \cdot N_E \quad (44)$$

The average molecular weights of process streams are used to relate mass and molar flow rates that were interchangeably used throughout this model and can be estimated by considering their major components. Mass and molar flow rates are related by the following relations

$$M_S = N_S \cdot MW_S \quad (45)$$

$$M_P = N_P \cdot MW_P \quad (46)$$

$$M_X = N_X \cdot MW_X \quad (47)$$

$$M_H = N_H \cdot MW_H \quad (48)$$

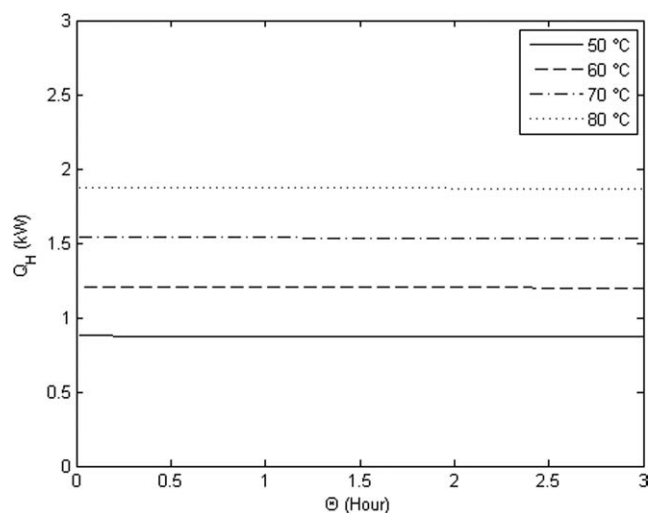


Figure 6. Heater load at several flash temperatures.

$$M_E = N_E \cdot MW_E \quad (49)$$

$$M_W = N_W \cdot MW_W \quad (50)$$

$$M_C = N_C \cdot MW_C \quad (51)$$

$$M_C^a = N_C^a \cdot MW_C^a \quad (52)$$

Correlations for enthalpy,¹⁷ density,¹⁸ and viscosity¹⁹ are included in the model to estimate stream properties as functions of temperature and salinity.

The model is now complete and a corresponding computer code is used to carry out different simulations of the process using several inputs of the controlling variables.

Results

A TK SolverTM computer code was developed to simultaneously solve the above equations in conjunction with the aforementioned correlations to estimate the physical proper-

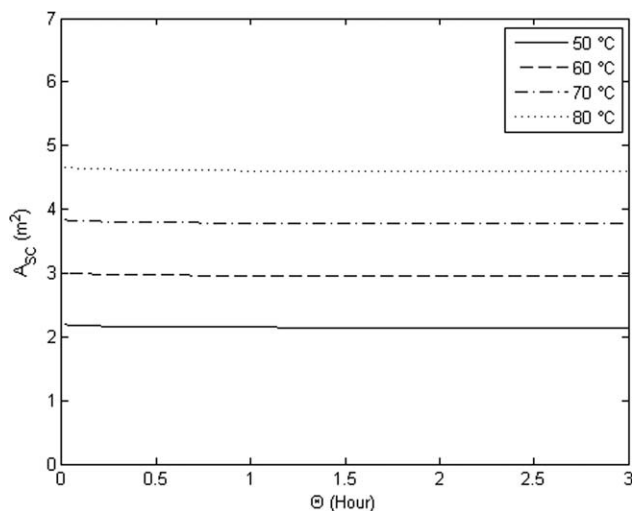


Figure 7. Solar collection area at several flash temperatures.

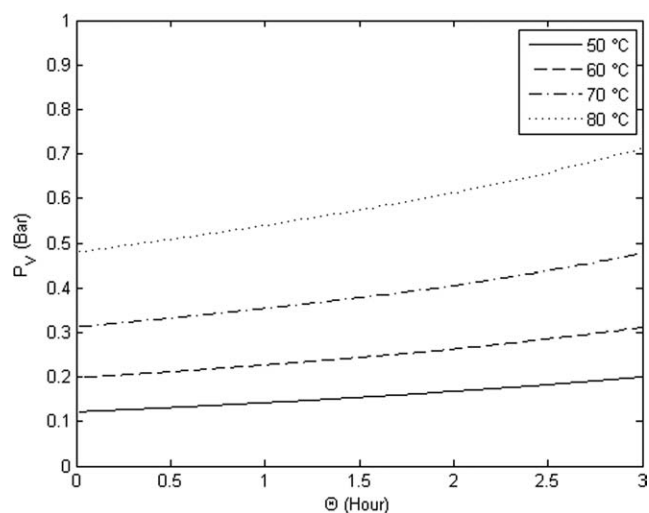


Figure 8. Vacuum pressure at several flash temperatures.

ties of the involved species and other operational parameters of the proposed system. Solution algorithm is iterative with 1 min long iterations. The following inputs were supplied to the code: $F_R = 0.82$; $I = 600 \text{ W/m}^2$; $M_S = 500 \text{ g/min}$; $T_E = 50, 60, 70, 80^\circ\text{C}$ (alternating input); $T_A = 25^\circ\text{C}$; $T_S = 25^\circ\text{C}$; $U = 0.92 \text{ W/m}^2 \text{ }^\circ\text{C}$; $\alpha = 0.92$; $\Theta = 0\text{--}180 \text{ min}$ (array input); $\tau = 0.90$; $\Phi_S = 0.035$.

In addition, conservative estimates of geometrical specifications, such as pipe length, pipe diameter, tank length, tank diameter, equipment elevations, and initial tank levels, were supplied to the code. The molecular weight of the involved species and the initial composition of seawater were also supplied to the code. The feed pump was assumed to be 1 HP and 70% efficient. Initial guesses for T_P , T_X , T_C , M_W , N_W , and NEA were also supplied. A General solution algorithm is outlined in Figure 5.

Discussion

Operating the unit under elevated flash temperatures will increase the energy of all the streams around the flash

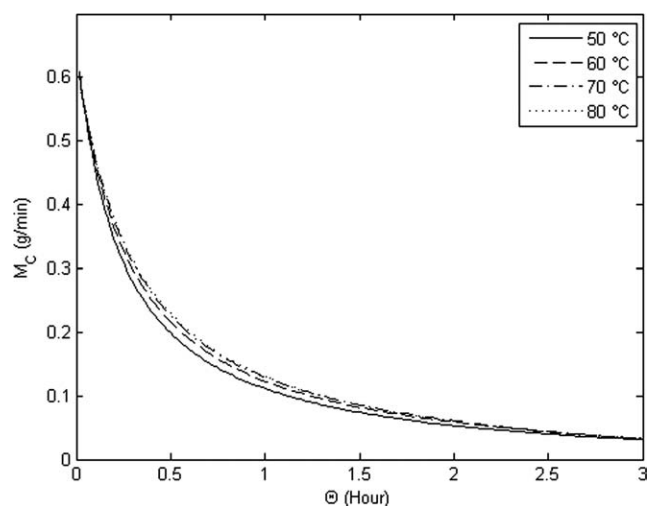


Figure 9. Production rate at several flash temperatures.

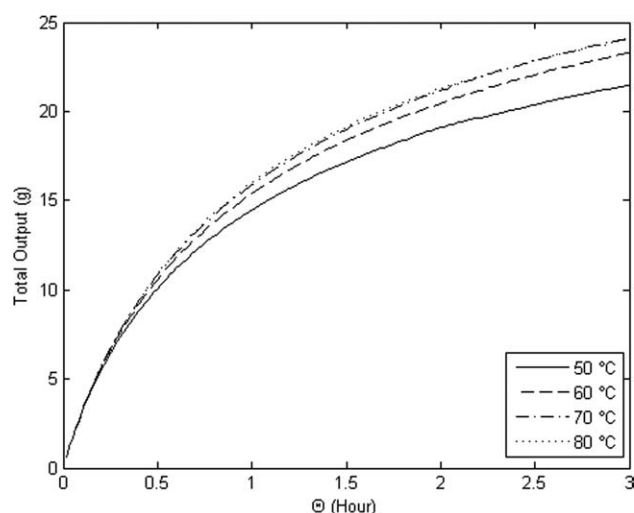


Figure 10. Production amount at several flash temperatures.

chamber according to the energy balance above. The higher energy demand is supplied by the solar heater; therefore, increasing the flash temperature will increase the heater load, as shown in Figure 6, and the required solar collection area, as shown in Figure 7. In addition, the heater load is gradually decreasing with time because of a declining energy demand for flashing caused by the slowly eroding vacuum; therefore, the heater load and the required solar collection area slightly decrease with time at a given constant flash temperature, as shown in Figures 6 and 7, respectively.

System pressure is directly proportional to temperature as expressed by all equations of state; accordingly, increasing the flash temperature will also increase the vacuum pressure as shown in Figure 8. In addition, flash chamber vacuum is continually eroding because of the build up of noncondensable gases. Continuous flash desalination systems include procedures to halt the operation, vent out the noncondensable gases, and resume under the regenerated vacuum.

Operating the unit under elevated flash temperatures will increase the overall vaporization of seawater in compliance with the thermodynamic phase equilibria. The increased vaporization gained from higher flash temperatures leads to more fresh water production rates as shown in Figure 9. In addition, fresh water production rates progressively decline because of the reduced flash vaporization attributed to the eroding vacuum. The cumulative effect of flash temperature on the total fresh water output, $M_C \times \theta$, is shown in Figure 10.

The hot concentrated brine subsequent to flashing represents a relatively large heat reservoir that can be tapped into to increase the thermal efficiency of the desalination unit. Using the multistage scheme mentioned earlier or using the concentrated brine to preheat the seawater feed stream seem to be viable options to reclaim part of that spent heat.

Conclusions

The proposed passive vacuum solar flash desalination process was simulated with a comprehensive computer model

using the fundamental physical and thermodynamic relationships to depict the process and several empirical correlations to estimate the physical properties of the involved species and the operational parameters of the proposed system.

The proposed desalination system is very energy efficient because it does not require high flash temperatures as it operates under vacuum; moreover, solar radiation is used in the heating module. In addition, the vacuum is naturally created by the hydrostatic forces without the need for vacuum pumps, making the unit even more energy efficient.

Running the system under higher flash temperatures will increase the heater load demanding more solar collection area; however, it will increase the fresh water output. Higher flash temperatures also entail faster vacuum erosion and shorter run time because the vacuum has to be recreated more often. Experimental replication of the proposed system is currently underway to validate model assumptions and predictions.

Notation

- $1/S$ = integrator
- A = area (m^2)
- BPE = boiling point elevation ($^{\circ}\text{C}$)
- E = energy flow (J/min)
- EOS = equation of state
- F = solar collector heat removal factor
- H = enthalpy (J/g)
- HC = Henry's constant (bar)
- HF = Henry's coefficient ($^{\circ}\text{C}$)
- HSS = high signal selector
- I = incident insolation on solar collector (W/m^2)
- K = vapor-liquid equilibrium distribution coefficient
- M = mass flow rate (g/min)
- MEB = mass and energy balance
- MW = molecular weight (g/mol)
- N = mole flow rate (mol/min)
- NEA = nonequilibrium allowance ($^{\circ}\text{C}$)
- P = pressure (bar)
- PA = vapor pressure coefficient
- PB = vapor pressure coefficient ($^{\circ}\text{C}$)
- PC = vapor pressure coefficient ($^{\circ}\text{C}$)
- Q = heat input (J/min)
- R = universal gas constant ($\text{bar cm}^3/\text{mol } ^{\circ}\text{C}$)
- T = temperature ($^{\circ}\text{C}$)
- U = solar collector heat loss conductance ($\text{W}/\text{m}^2 \text{ } ^{\circ}\text{C}$)
- v = mole fraction in condensed water
- V = volume (cm^3)
- VPC = vapor pressure correlation
- W = work output (J/min)
- x = mole fraction in concentrated brine
- y = mole fraction in flashed vapor
- z = mole fraction before flash
- α = K -value correction factor/solar collector absorptance
- θ = run time (min)
- τ = solar collector transmittance
- ϕ = stream mass fraction
- ω = salt mass fraction

Subscripts

- A = ambient
- BP = bubble point
- C = condenser
- DP = dew point
- E = evaporator
- H = heater
- P = pump
- S = seawater

Salt = seawater salt
 SC = solar collector
 R = solar collector heat removal factor
 V = vacuum
 W = brine
 X = Preheat

Superscripts

° = reference state
 a = accumulated
 C = condenser
 E = evaporator
 i = initial state
 in = entering
 L = latent
 out = existing
 sat = saturation.

Literature Cited

1. Culp A. *Principles of Energy Conversion*. New York: McGraw Hill, 1991.
2. Al-Kharabsheh S, Goswami DY. Analysis of an innovative water desalination system using low-grade solar heat. *Desalination*. 2003;156:323–332.
3. Al-Kharabsheh S. Theoretical and Experimental Analysis of Water Desalination System Using Low Grade Solar Heat. PhD Dissertation, University of Florida, Gainesville, FL, 2003.
4. Maroo SC. Theoretical Analysis of Solar Driven Flash Desalination System Based on Passive Vacuum Generation. MS Thesis, University of Florida, Gainesville, FL, 2006.
5. Goswami DY, Kreith F, Kreider JF. *Principles of Solar Engineering*, 2nd ed. Philadelphia, PA: Taylor & Francis, 2000.
6. Hermann M, Koschikowski J, Rommel M. Corrosion-free solar collectors for thermally driven seawater desalination. *Solar Energy*. 2002;72:415–426.
7. Turekian KK. *Oceans*. Englewood Cliffs, NJ: Prentice Hall, 1968.
8. Sander R. Compilation of Henry's law constants for inorganic and organic species of potential importance in environmental chemistry. Available at: www.henrys-law.org, 1999.
9. Geankoplis CJ. *Transport Processes and Separation Process Principles*. Englewood Cliffs, NJ: Prentice Hall, 2003.
10. Perry RH, Green D. *Perry's Chemical Engineers' Handbook*. New York: McGraw Hill, 1984.
11. Thibodeaux LJ. *Environmental Chemodynamics*. New York: Wiley, 1996.
12. Rachford HH, Rice JD. Procedure for Use of Electronic Digital Computers in Calculation Flash Vaporization Hydrocarbon Equilibrium. *Petroleum Technology* 1952;195:327–337.
13. Granet I. *Fluid Mechanics*. Englewood Cliffs, NJ: Prentice Hall, 1996.
14. Bemporad GA. basic hydrodynamic aspects of a solar energy based desalination process. *Solar Energy*. 1995;54:125–134.
15. El-Nashar AM, Qamhiyeh AA. Simulation of the steady-state operation of a multi-effect stack seawater distillation plant. *Desalination*. 1995;101:231–243.
16. Miyatake O, Murakami K, Kawata Y, Fujii T. Fundamental experiments with flash evaporation. *Heat Transfer-Jpn Res*. 1973;2:89–100.
17. Connors DN. On the enthalpy of seawater. *Limnol Oceanogr*. 1970;15:587–594.
18. Millero FJ, Poisson A. International one-atmosphere equation of state of seawater. *Deep Sea Res*. 1981;28:625–629.
19. Sündermann J. Landolt-Börnstein: Numerical Data and Functional Relationships in Science and Technology. Group V: Geophysics and Space Research, Vol. 3: Oceanography. Sub-Volume: A. Berlin, Germany: Springer, 1986.

Manuscript received Nov. 24, 2008, and revision received July 22, 2009.